European Journal of Pharmaceutics and Biopharmaceutics 80 (2012) 443–452

Contents lists available at SciVerse ScienceDirect

European Journal of Pharmaceutics and Biopharmaceutics

journal homepage: www.elsevier.com/locate/ejpb

Research paper

Dissolution of a poorly water-soluble drug dry coated with magnesium and sodium stearate

Tracy Tay [a], David A.V. Morton [a], Thomas R. Gengenbach [b], Peter J. Stewart [a,*]

[a] Drug Delivery, Disposition and Dynamics, Monash Institute of Pharmaceutical Sciences, Monash University, Victoria, Australia
[b] CSIRO Materials Science and Engineering, Bayview Avenue, Victoria, Australia

ARTICLE INFO

Article history:
Received 22 June 2011
Accepted in revised form 11 October 2011
Available online 20 October 2011

Keywords:
Mechanical dry particle coating
Mechanofusion
Dissolution
Poorly water-soluble drugs
Magnesium stearate
Sodium stearate

ABSTRACT

The purpose of this research was to investigate the influence of dry coating micronized cohesive powders of a poorly water-soluble drug, indomethacin with force control agents, on its dissolution performance. A dry mechanical fusion method (mechanofusion) was used to coat indomethacin powders with magnesium stearate (0.25%, 1%, 5%) and sodium stearate (5%). After mechanofusion, significantly increased bulk and tapped densities and decreased intrinsic cohesion were observed for all samples. X-ray photoelectron spectroscopy analysis confirmed that a thicker magnesium stearate surface coating was achieved with increasing concentrations of the material. Dissolution was studied using the USP paddle method in buffer pH 5.0; several modelling approaches were used to explore the dissolution mechanisms. Whilst the bi-exponential equation represented dissolution of mechanofused indomethacin powders occurring from dispersed and agglomerated particles, it provided unrealistic parameter estimates for the two coating materials of contrasting properties. Initial increases in indomethacin dissolution were dependent on the concentration of magnesium stearate mechanofused onto the drug powders. The dissolution enhancing effect of indomethacin powders mechanofused with 5% sodium stearate was attributed to its surfactant properties that increased dispersion of indomethacin agglomerates. Initial drug release from the coated powders was described by a matrix-diffusion system according to the Higuchi model.

1. Introduction

Poorly water-soluble drugs are often micronized to improve their dissolution rate through increasing the surface area available to the dissolution medium. However, the intrinsic cohesion of such fine drug powders is problematic as they tend to form agglomerates; the effectively reduced surface areas result in incomplete dispersion of the drug in the gastrointestinal fluids and consequently a deleterious effect on its dissolution performance [1].

The efficiency of the dispersibility of a powder/liquid system is known to decrease as the powder cohesiveness increases [2], i.e. the attractive forces between primary particles of agglomerates must be overcome by gravitational forces to enable dispersion. For micron and sub-micron sized particles, the dominating inter-particle cohesive force is the van der Waals force [3], the magnitude of which decreases sharply with an increase in the separation distance between two particles [4].

In recent years, highly intensive mechanical dry particle coating approaches (generically termed "mechanofusion") have been used to effectively modify the interparticulate interactions of dry powders by changing their surface characteristics [5,6]. This technique which coats particles through a mechano-chemical fusion reaction provides a more uniform and hence more effective coating than possible via conventional blending particularly for cohesive powders [7]. A number of different mechanofusion systems are available and in general, they consist of a rotating cylindrical chamber (with relatively high speeds, i.e. up to 5000 rpm) in which both a fixed rounded inner-piece working head (stator) and scraper blade are placed. When a measured amount of host and guest particles are added into the rotating vessel, the powder is forced out towards the chamber walls by centrifugal action. Since the gap between the inner-piece and rotating drum is controlled, the particles passing through the gap are subjected to intense friction, shearing and compressive forces. As a result of a considerable amount of thermo-mechanical energy that is generated through these forces, the guest material is coated onto the exposed surfaces of the host particles due to the very strong physical and/or chemical bonds that form [6,8,9].

The majority of applications of dry particle coating within the pharmaceutical arena have focused on enhancing the dispersibility of powders for inhalation. Optimum cohesive-adhesive balance is achieved through the use of low surface energy materials known as force control agents (FCAs) that exhibit anti-adherent and anti-friction properties. FCA materials (including amino acids such as

* Corresponding author. Drug Delivery, Disposition and Dynamics, Monash Institute of Pharmaceutical Sciences, Monash University, 381 Royal Parade, Parkville, Victoria 3052, Australia. Tel.: +61 3 9903 9517; fax: +61 3 9903 9583.
E-mail address: peter.stewart@monash.edu (P.J. Stewart).

0939-6411/$ - see front matter © 2011 Elsevier B.V. All rights reserved.
doi:10.1016/j.ejpb.2011.10.009

leucine, phospholipids such as lecithin, or fatty acid derivatives such as magnesium stearate and sucrose tristearate) have been shown to facilitate the de-agglomeration of cohesive powders in carrier-based formulations [10–13]. The mechanical fusion of FCAs significantly influences the forces between drug particles and results in nanometre-thick coatings of host particles [10]. Dispersibility of the cohesive drug powders is achieved through increased detachment from carriers and de-agglomeration [14,15]. Begat et al. [10,13] also attempted to coat the drug rather than the carrier particles with FCAs; this led to substantially enhanced de-agglomeration and dispersion of the respirable particles.

To date, few studies have addressed the dissolution of such dry coated materials. The dissolution of drugs embedded into a carrier particle by mechanofusion has been studied. For example, when various micronized poorly water-soluble drugs (including oxyphenbutazone, prednisolone, theophylline, indomethacin, phenacetin and aspirin) were dry coated onto coarse starch particles, marked improvements in drug dissolution were found from the resultant drug-diluent hybrid powders [16–18]; these enhancements were attributed to increases in both the drug wettability and surface area available for dissolution. Also, embedding naproxen in porous starch by mechanofusion produced faster rates of drug dissolution compared with the physical mixtures [19].

No previous studies have been found by the authors that have utilized the approach of dry coating the drug (rather than the carrier particle) with a guest material motivated to improve its dissolution performance. The primary aim of this study was to therefore investigate the effect of dry coating micronized cohesive powders of a model poorly water-soluble drug, indomethacin with FCAs on its dissolution rate. Two fatty acid salts, magnesium stearate and sodium stearate, were selected as the FCAs for their contrasting hydrophobic and hydrophilic properties, respectively [20,21]. These materials are known to be effective boundary lubricants owing to their high melting points and capability of being strongly adsorbed onto a surface to form films of low shear strength [22,23]. The coated powders were characterized by their intrinsic cohesion, and the surface composition was analysed by X-ray photoelectron spectroscopy (XPS). Dissolution of the indomethacin powders, both untreated and coated with FCAs, was determined using a conventional USP paddle method and the data modelled to investigate the influence of coating on the release mechanism of dissolved indomethacin.

2. Materials and methods

2.1. Materials

Indomethacin, IMC (Wuhan Yuancheng Technology Development Co. Ltd., Wuhan, Hubei, China), was micronized (D_{10} = 0.9 μm, D_{50} = 2.4 μm, D_{90} = 5.5 μm) and used as the model drug. The materials investigated as FCAs were magnesium stearate, MgSt (D_{10} = 2.6 μm, D_{50} = 7.5 μm, D_{90} = 15.8 μm) (Mallinckrodt Baker Inc., Phillipsburg, NJ, USA), and sodium stearate, NaSt (D_{10} = 2.6 μm, D_{50} = 10.2 μm, D_{90} = 30.8 μm) (Sigma–Aldrich, St. Louis, MO, USA).

2.2. Particle size analysis

Primary particle size distributions (PSD) of IMC and the FCA materials were determined by laser diffraction using a Scirocco cell and Scirocco 2000 dry powder feeder (Mastersizer 2000; Malvern Instruments Ltd., Worcestershire, UK). Approximately 10–30 mg of each powder sample was dispersed in air at a pressure of 400 kPa. All measurements were performed on the basis of five replicates for each sample and were between an obscuration of 1 and 5%. The different optical characteristics of the various materials were also taken into account by including their refractive index (RI) values during analysis; reference RIs of 1.74, 1.525 and 1.00 were used for IMC, the FCA materials (MgSt and NaSt) and air as the dry dispersant, respectively, with an estimated imaginary RI of 0.01. Average PSDs were characterized by the D_{10}, D_{50} and D_{90} cumulative particle undersize values.

2.3. Preparation of powder formulations

2.3.1. Micronization

Powders of IMC were micronized in an air-jet mill (Trost Air Impact Pulveriser; Trost Equipment Corporation, Newtown, PA, USA). The material was manually fed into the milling inlet at an approximate rate of 100 g/h using a grinding air pressure of 680 kPa and a feed pressure of 280 kPa.

2.3.2. Mechanical dry coating of indomethacin powders

Drug powders of IMC were dry coated with MgSt and NaSt using an AMS-Mini mechanofusion system with a Nobilta process module (Hosokawa Micron Corporation, Osaka, Japan). Each formulation (10 g batches prepared in duplicate) comprising IMC and either MgSt (0.25%, 1%, 5% w/w) or NaSt (5% w/w) was directly weighed into the processing chamber of the mechanofusion setup and sealed. Mains water supply was circulated through an incorporated cooling jacket in order to prevent the vessel temperature from exceeding 25 °C over the course of the mechanofusion process. An initial pre-blend of the powders was performed at a paddle speed of 500 rpm for 5 min; the speed was then steadily increased to 5000 rpm over 2 min and maintained at that speed for a further 10 min to mechanically fuse the FCA onto the micronized drug. A nylon brush was used to remove the powder layer attached on the chamber wall at every 2 min interval of the process.

After mechanofusion, all resulting powders were passed through a stainless steel sieve (Labtechnics, Kilkenny, SA, Australia) with an aperture size of 355 μm to ensure uniformity of the particle size characteristics for dissolution testing.

2.4. Powder density

The untreated and mechanofused IMC powders were gently poured into a calibrated 10 ml measuring cylinder through a funnel placed at a fixed height directly above it. The ratio of the mass of powder to the volume that it occupied in the cylinder was referred to as its bulk density (g/ml). The filled cylinder was then placed onto an automatic tapper (Model AT-2 AUTOTAP Tap Density Analyzer; Quantachrome Instruments, Boynton Beach, FL, USA) and mechanically tapped 1000 times at a rate of 260 taps/min. The powder volume occupied by the cylinder after tapping was subsequently used to calculate its tapped density (g/ml). All measurements were averaged from three replicates for each sample.

2.5. Cohesion and shear testing

The cohesion and shear strength properties of the mechanofused powders were characterized using the small-scale shear test module of the FT4 powder rheometer (Freeman Technology, Worcestershire, UK). A shear head was attached to the powder rheometer unit and shear stress was measured with respect to a given consolidating normal stress. Subsequent shear tests were carried out at normal stresses of 7, 6, 5, 4 and 3 kPa; yield loci were then derived as curves to represent the maximum shear stress the sample can support under a certain normal stress. The shear strength provides a measure of the force required to shear the powder sample and is therefore indicative of the strength of the interparticle forces. In addition, the cohesion of each sample was determined

by extrapolating the yield loci to zero normal stress. Measurements of all samples were performed in triplicate and were preconditioned using the instrument's condition methodology.

2.6. X-ray photoelectron spectroscopy (XPS)

X-ray photoelectron spectroscopy (XPS) analysis was performed with an AXIS HSi Spectrometer (Kratos Analytical Ltd., Manchester, UK), equipped with a monochromated Al K_∞ source at a power of 144 W (12 kV × 12 mA). A small quantity of each sample was filled into shallow wells of custom-made powder sample holders. Charging of the samples during irradiation was compensated by an electron flood gun in combination with a magnetic immersion lens. A reference binding energy of 285 eV for the aliphatic hydrocarbon C 1s component was used to correct for any remaining offsets due to charge neutralization of specimens under irradiation. The pressure in the main vacuum chamber during analysis was typically 1×10^{-6} Pa. Spectra were recorded with the nominal photoelectron detection normal to the sample surface. For each sample that was prepared, analysis was undertaken at two different locations at a nominal photoelectron emission angle of 0° with respect to the normal surface. Since the actual emission angle is ill-defined in the case of powders, the sampling depth may vary between 0 and 10 nm depending on the kinetic energy of the measured photoelectrons.

All elements present were identified from survey spectra (acquired at a pass energy of 320 eV). For further analysis, high resolution spectra were recorded from individual peaks at 40 eV pass energy (yielding a typical peak width for polymers of 1.0–1.1 eV). The atomic concentrations of the detected elements were calculated using integral peak intensities and the sensitivity factors supplied by the instrument manufacturer. The accuracy associated with quantitative XPS is ca. 10–15%. The precision depends on the signal/noise ratio and is generally assumed to be in the order of 1–5% for more abundant elements. The latter is more relevant when comparing samples of similar composition.

2.7. Scanning electron microscopy

The untreated and mechanofused IMC powders were examined at several magnifications under a Phenom scanning electron microscope (FEI Company, Eindhoven, the Netherlands), operated at 5 kV. Prior to analysis, powder samples were mounted on aluminium stubs using carbon coated adhesive tabs and then gold coated with a sputter coater (K550X sputter coater; Emitech Ltd., Ashford, Kent, UK) equipped with an Edwards RV3 vacuum pump (Edwards Vacuum Ltd., Crawley, West Sussex, UK) at 20 nm thickness.

2.8. In vitro dissolution studies

Dissolution of the untreated and mechanofused IMC powders was conducted with an automated dissolution apparatus consisting of a six vessel constant temperature bath (Erweka DT6; Erweka, Heusenstamm, Germany) and multichannel peristaltic pump (IPC 8 Ismatec® pump; Ismatec SA, Glattbrugg, Switzerland) equipped with an online ultraviolet (UV) spectrophotometer (Cecil CE 3021; Cecil Instruments Ltd., Cambridge, UK) which contained 10 mm flow cells. The USP Dissolution Apparatus 2 paddle method (United States Pharmacopeia 32/National Formulary 27, 2009) was used at a rotational speed of 100 rpm. The dissolution medium (1000 ml) consisted of an acetate buffer pH 5.0 (British Pharmacopoeia 2009) (995 ml) and 0.1% w/v sodium lauryl sulphate solution (Sigma, Castle Hill, NSW, Australia) (5 ml) to improve drug wettability. Prior to use, all dissolution media were freshly degassed through a 0.45 μm membrane filter (Millipore Corporation, Bedford, MA, USA) and equilibrated to 37.0 ± 0.5 °C in the dissolution bath. Powder samples were then added to the six dissolution vessels in series, yielding a theoretical drug concentration of 3 mg/l in each vessel to give sink conditions. Upon automatic sampling, absorbance readings (six replicates) for IMC were recorded at the wavelength of maximum absorption at two minute intervals over a period of 60 min.

The amount of IMC dissolved (%) at each time interval was calculated from the mean drug content using a validated UV assay (Section 2.9), which was based on five replicates per mixture.

2.9. UV analysis of indomethacin

A UV–visible spectrophotometer (Cecil CE 3021; Cecil Instruments Ltd., Cambridge, UK) was used to analyse the IMC content from the dissolution studies. The wavelength of maximum absorption of IMC, determined over a wavelength range of 200–500 nm at a concentration of 5.0 μg/ml, was 265.4 nm in acetate buffer pH 5.0. The Beer's law calibration plot for IMC in the dissolution medium at 265.4 nm was constructed using three replicates over six concentrations (from 0.5 to 3.0 μg/ml), which was within the solubility range of the drug to achieve sink conditions. No deviation from linearity was observed ($R^2 = 1.000$) and the intercept was not significantly different from zero ($P > 0.05$). Over low, medium and high concentrations of IMC, the accuracy and precision of the assay ranged from 98.5–99.9% of the theoretical concentration and the coefficient of variation was ⩽3.8%, respectively.

2.10. Dissolution modelling

Dissolution data were modelled using a non-linear least squares regression analysis based on the Levenberg–Marquardt algorithm [24,25] in order to estimate the coefficients or parameters of the independent variables that provide the best fit between the equation and the data (SigmaPlot® 11.0; Systat Software Inc., San Jose, CA, USA). The average undissolved concentrations (%) of IMC versus time data were modelled using multi-exponential equations, where each exponential term represented the dissolution of a discrete distribution of either dispersed drug particles or agglomerates. The equations describing single (2 parameter), double (4 parameter) and triple (6 parameter) decay equations are shown below (Eqs. (1)–(3)):

$$C = C_d \exp(-k_d t) \quad (1)$$

$$C = C_d \exp(-k_d t) + C_a \exp(-k_a t) \quad (2)$$

$$C = C_d \exp(-k_d t) + C_{a1} \exp(-k_{a1} t) + C_{a2} \exp(-k_{a2} t) \quad (3)$$

where C is the concentration of the undissolved drug (%) at time t; C_d and C_a are the initial concentrations (%) of dispersed particles and agglomerates, respectively, with their corresponding dissolution rate constants k_d and k_a (min^{-1}). In cases where more than one agglomerate distribution occurs, a tri-exponential equation (Eq. (3)) involves two agglomerate size populations designated as a1 and a2. These exponential terms represent dissolution from distributions of "dispersed" and "agglomerated" particles; the former has a greater influence on dissolution because of surface area effects.

Discrimination between the competing models to assess the goodness of fit was performed on the basis of several statistical parameters: correlation coefficient (R^2) (a value close to 1 indicates a greater degree of correlation and hence more favourable), F-statistic (assesses the improved fit with the use of additional parameters where a greater value implies a better fit), Norm value (square root of the sum of squares in which a smaller value provides a superior fit of the data), Akaike Information Criterion

(AIC) (provides a measure of goodness of fit based on maximum likelihood by relating the weighted residual sum of squares to the number of parameters that were required to obtain the fit; the model yielding the smallest value is the most suitable one) and dependency values (an indication of model complexity where a value close to 1 indicates over-parameterization).

2.11. Statistical analysis

Data were statistically analysed to compare differences between groups of values using one-way analysis of variance (ANOVA) with a post-hoc Tukey's test (PASW Statistics 17.0; IBM Corporation, Somers, NY, USA). Probability values (P) of less than 0.05 were considered as statistically significant.

3. Results

3.1. Powder densities and particulate interactions

Following mechanofusion of the IMC powders with MgSt (0.25%, 1%, 5%) and NaSt (5%), the samples were characterized in terms of their densities, shear stress-normal stress plots and cohesion properties. These results are discussed below.

The density of the powder samples is presented in Fig. 1. Both the bulk and tapped densities of all mechanofused samples were significantly higher than those of the untreated IMC ($P \leqslant 0.002$). The greatest change in density was found after mechanofusion with 5% MgSt, as noted by increases of 84.8% and 94.9% for the bulk (0.35 ± 0.01 g/ml) and tapped (0.64 ± 0.01 g/ml) densities, respectively, from those of the untreated IMC (0.19 ± 0.00 and 0.33 ± 0.01 g/ml) ($P < 0.001$). More interesting to note was an increasing trend in the densities (bulk and tapped) with MgSt concentration, where the densities between all MgSt samples (0.25–5%) were found to be significantly different ($P < 0.001$). The 5% NaSt-IMC sample exhibited similar densities with those of the 1% MgSt-IMC sample ($P > 0.05$). The very low bulk density of the untreated micronized drug powders was an indication of a high porosity in which particles and agglomerates existed as loose open packed structures held together by the interactive forces. Even after compression by mechanical tapping, the particles and agglomerates were not able to pack tightly. However, the marked increases in densities following surface treatment of IMC demonstrated an improved packing efficiency of the powders, reducing the voidage spaces between the particles. This change in packing fraction may be ascribed to a reduced interparticulate interaction and changes in the particle surface characteristics, composition and morphology due to the coating and deformation effects caused by mechanofusion processing.

Shear stress-normal stress profiles and the intrinsic cohesion properties of the powder samples before and after mechanofusion were evaluated and the results shown in Figs. 2A and B. As seen from the shear stress-normal stress profiles, the untreated IMC and mechanofused samples with 0.25% and 1% MgSt exhibited the highest shear stress values at each normal stress (Fig. 2A). In contrast, mechanofusion with 5% MgSt produced much lower shear stress values than those of the other samples at all normal stresses ($P < 0.001$). Upon extrapolation of the yield loci to zero normal stress, the derived cohesion values were consistent with the trends observed from the above profiles. For example, the untreated IMC demonstrated the highest cohesion of 4.13 ± 0.28 kPa and was not significantly different from the values for both the 0.25% and 1% MgSt-IMC samples ($P > 0.05$) (Fig. 2B). Although the yield locus of the 5% NaSt-IMC sample was similar to those of the untreated

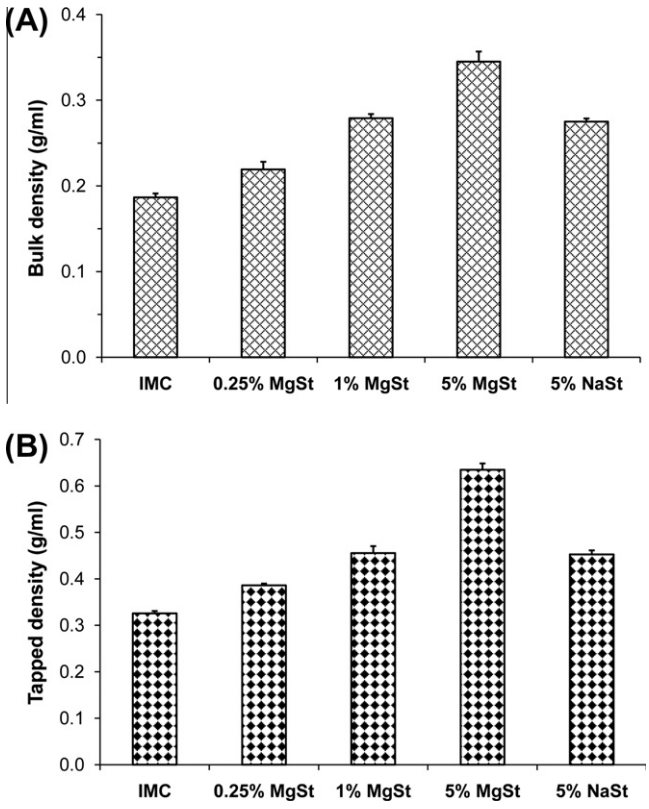

Fig. 1. Changes in the (A) bulk and (B) tapped densities for untreated indomethacin (IMC) and IMC powders mechanofused with magnesium stearate (MgSt; 0.25–5%) and sodium stearate (NaSt; 5%) ($n = 3$).

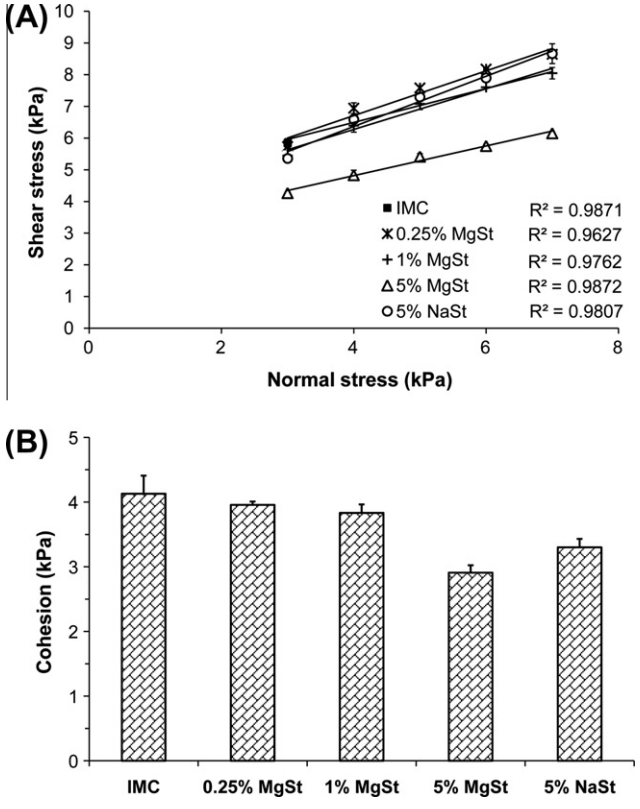

Fig. 2. (A) Shear stress-normal stress profiles and (B) cohesion results for the untreated indomethacin (IMC) and IMC powders mechanofused with magnesium stearate (MgSt; 0.25–5%) and sodium stearate (NaSt; 5%), measured by the FT4 powder rheometer in its shear mode ($n = 3$).

Table 1
XPS surface composition of mechanofused indomethacin (IMC) with magnesium stearate (MgSt), expressed as atomic ratios relative to total carbon.

	IMC	0.25% MgSt	1% MgSt	5% MgSt	MgSt
O/C	0.198 ± 0.006	0.185 ± 0.000	0.158 ± 0.001	0.107 ± 0.002	0.099 ± 0.001
N/C	0.051 ± 0.001	0.053 ± 0.001	0.040 ± 0.001	0.018 ± 0.001	0.002 ± 0.002
Cl/C	0.050 ± 0.000	0.046 ± 0.001	0.039 ± 0.001	0.013 ± 0.001	
Mg/C		0.003 ± 0.000	0.010 ± 0.001	0.022 ± 0.000	0.032 ± 0.001

IMC and mechanofused 0.25% and 1% MgSt-IMC samples, the difference in the slope gave a similar cohesion value to that of the 5% MgSt-IMC sample ($P = 0.08$); the cohesion values for the 5% MgSt-IMC and NaSt-IMC samples were substantially lowered to 2.91 ± 0.11 and 3.30 ± 0.13 kPa, respectively ($P \leqslant 0.001$).

3.2. Surface composition

X-ray photoelectron spectroscopy (XPS) was used to quantitatively analyse the surface elemental composition of the coated particles after mechanofusion. Atomic concentrations of all elements detected on the sample surfaces (O, N, Cl, Mg or Na) were determined and converted to atomic ratios (atomic concentrations relative to the total concentration of carbon, i.e. X/C). Comparison of these elemental atomic ratios for the mechanofused samples relative to those for pure IMC, MgSt and NaSt would enable determination of the quantity of the particular FCA present on the IMC surfaces.

The surface elemental composition for the pure materials and mechanofused samples expressed in terms of the O/C, N/C and Cl/C, Mg/C and Na/C atomic ratios is presented in Tables 1 and 2. The measured values for the pure materials were compared to their corresponding theoretical stoichiometric ratios (Table 3). The surface elemental compositions (of O, N, Cl and Mg or Na) for pure IMC, MgSt and NaSt were calculated to be within 94–96%, 89–114% and 92–114%, respectively, of their theoretical stoichiometric values. These results indicated a high level of purity for the above listed materials.

In the case of the mechanofused samples, the results revealed that the elemental surface concentrations changed with the concentration of the FCA, i.e. with increasing MgSt concentrations, the elemental ratios of the mechanofused samples had shifted closer to those values representing pure MgSt relative to that of IMC (Table 1). For example, the atomic ratios of O/C and N/C progressively decreased from 0.185 ± 0.000 and 0.053 ± 0.001, respectively, for the 0.25% MgSt-IMC sample to 0.107 ± 0.002 and 0.018 ± 0.001 after coating with 5% MgSt ($P < 0.001$); relative to the untreated IMC, the latter values were closer to the corresponding atomic ratios of 0.099 ± 0.001 and 0.002 ± 0.002 for pure MgSt. Similar trends were seen for Cl that was not present on the surface of pure MgSt. The significant decreases in the Cl/C atomic ratios between IMC and 0.25% MgSt-IMC and between all mechanofused samples ($P < 0.05$) correlated to lower surface concentrations of Cl and hence a thicker MgSt coating. These observations were confirmed with the analysis of elemental Mg. The pure MgSt material was high in Mg content compared to the untreated IMC (which did not contain any Mg), as noted by its Mg/C atomic ratio of 0.032 ± 0.001. Significant increases in the Mg/C atomic ratios with an increasing concentration of MgSt in the mechanofused samples (0.25–5%) ($P \leqslant 0.008$) and towards that of pure MgSt indicated that IMC particles were progressively coated with higher amounts of MgSt. Comparison between the Mg/C ratios demonstrated that around 70% of Mg was detected on the surface of the 5% MgSt mechanofused sample relative to that of the pure MgSt material.

Table 2
XPS surface composition of mechanofused indomethacin (IMC) with sodium stearate (NaSt), expressed as atomic ratios relative to total carbon.

	IMC	5% NaSt	NaSt
O/C	0.198 ± 0.006	0.142 ± 0.001	0.102 ± 0.001
N/C	0.051 ± 0.001	0.029 ± 0.000	
Cl/C	0.050 ± 0.000	0.025 ± 0.001	
Na/C		0.036 ± 0.000	0.064 ± 0.000

Table 3
Atomic ratios (elemental concentrations relative to the total concentration of carbon) for indomethacin (IMC), magnesium stearate (MgSt) and sodium stearate (NaSt), based on the theoretical stoichiometry.

	IMC	MgSt	NaSt
O/C	0.211	0.111	0.111
N/C	0.053		
Cl/C	0.053		
Mg/C		0.028	
Na/C			0.056

Analysis of the 5% NaSt-IMC sample also revealed that the IMC powders were coated with NaSt during the mechanofusion process (Table 2). For example, the O/C, N/C and Cl/C atomic ratios were significantly lower than the corresponding values for the untreated IMC ($P < 0.001$), indicating a lower contribution of IMC and a resultant higher content of NaSt on the powder surfaces. The calculated amount of elemental Na present on the surface of the mechanofused sample relative to that of pure NaSt was 56%; this was less than the amount of elemental Mg detected on the 5% MgSt-IMC sample surface and hence indicated a lower surface coverage of the FCA on the IMC powders. This conclusion is also consistent with the observation that O/C, N/C and Cl/C ratios were all lower for the 5% MgSt-IMC sample compared to those of the 5% NaSt-IMC sample. It should also be noted that for each cation, MgSt contains two stearate moieties compared to one stearate in the case of NaSt.

3.3. Surface characteristics and morphology

Imaging by scanning electron microscopy (SEM) was used to observe the surface morphology and surface quality of particles after coating. Representative SEM images of the FCA materials, untreated and mechanofused IMC powders are shown in Fig. 3. Particles of MgSt appeared as flake-shaped particles occurring as plate-like sheets (Fig. 3A), whilst those of NaSt exhibited flat tabular flake forms with some fines existing on the surfaces of the larger particles (Fig. 3B). SEMs of the untreated IMC powders were depicted as a dense network of agglomerated particles (Fig. 3C). Mechanofusion with 0.25% MgSt did not induce substantial changes in the agglomerate structure from that of the untreated sample, with particles remaining as cohesive agglomerated masses (Fig. 3D). However, noticeable differences were apparent with the use of higher concentrations of MgSt (5%), where the mechanofused

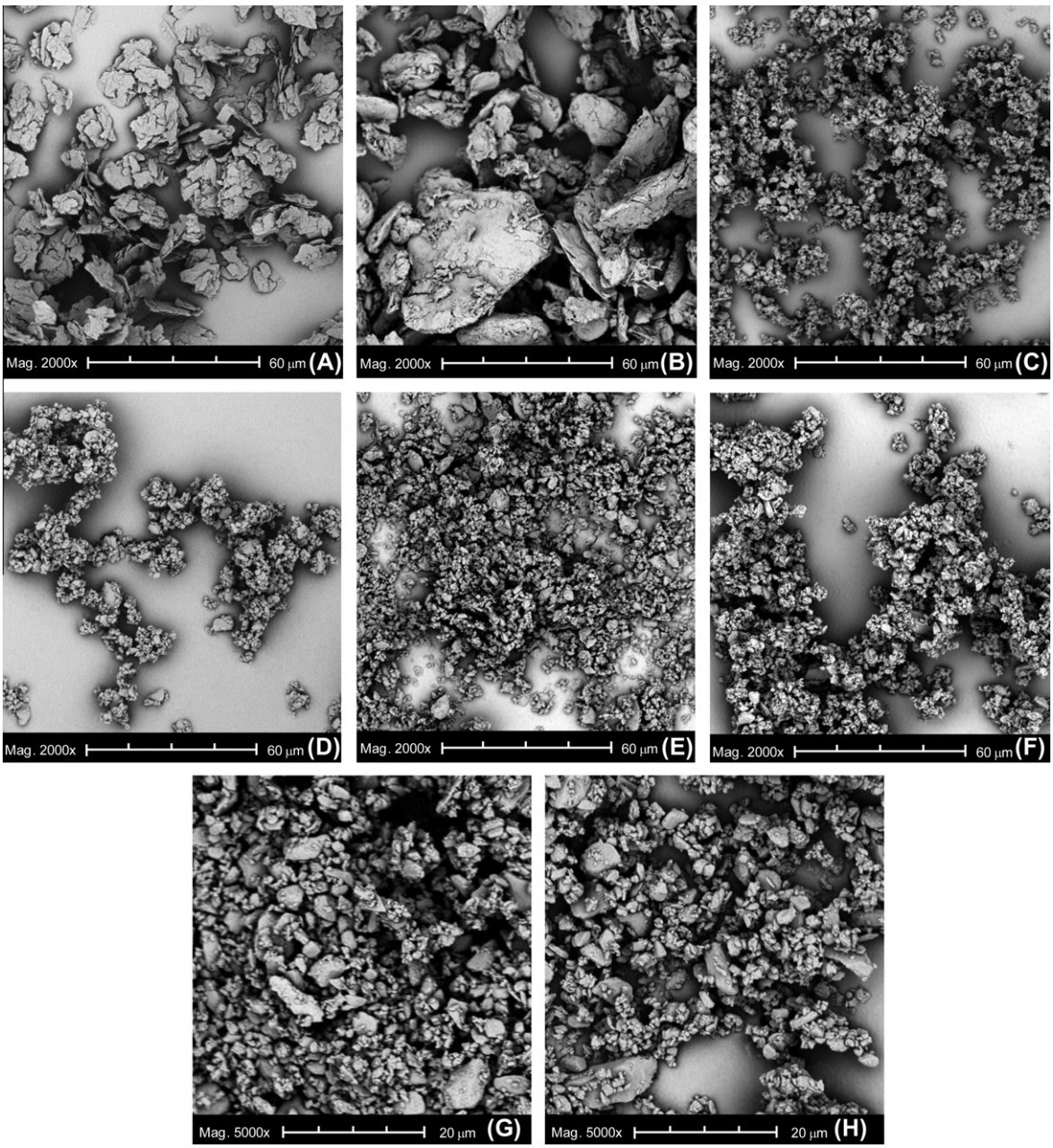

Fig. 3. Scanning electron micrographs of (A) magnesium stearate (MgSt), (B) sodium stearate (NaSt), (C) untreated indomethacin and indomethacin powders mechanofused with (D) 0.25% MgSt, (E, G) 5% MgSt and (F, H) 5% NaSt.

powders appeared much less agglomerated and were dispersed as more loosely open packed particles (Fig. 3E). On the other hand, finely agglomerated particles existed following surface treatment with 5% NaSt (Fig. 3F), similar to that of the 0.25% MgSt-IMC sample (Fig. 3D).

To complement the XPS data, a closer examination of the SEMs also assisted in an assessment of the coating efficiency of the two FCA materials. For the 5% MgSt-IMC sample (Fig. 3G), the absence of any flake-shape MgSt particles within these powders supported the intended outcome that particles of MgSt had been delaminated and spread over the surface of IMC particles during the highly intensive shear and compressive mechanofusion process; this phenomenon resembles the surface adsorption mechanism previously described by Shah and Mlodzeniec [26]. A magnified image of the IMC powders mechanofused with 5% NaSt (Fig. 3H) depicted the presence of larger particles (up to 15 μm in size) that were characteristic of the NaSt within the sample; this indicated that the FCA material was not coated onto the drug powder surfaces in a similar manner to that of the MgSt where a delamination mechanism was observed to occur (Fig. 3G).

3.4. Dissolution of mechanofused indomethacin

Dissolution profiles of the untreated and mechanofused IMC with MgSt (0.25%, 1%, 5%) and NaSt (5%) were determined in acetate buffer at pH 5.0 over 60 min (Fig. 4). The dissolution of each of these samples followed a biphasic pattern that was characteristic of a rapid initial dissolution phase, followed by a slower dissolution phase at later dissolution times. During the initial phase where most of the dissolution was occurring, the dissolution rate of IMC increased with MgSt concentration, i.e. the amount of IMC dissolved at 10 min significantly increased from 19.4 ± 2.1% for untreated IMC to 25.5 ± 1.7% after mechanofusion with 5% MgSt ($P < 0.001$). The use of both 0.25% and 1% MgSt did not yield

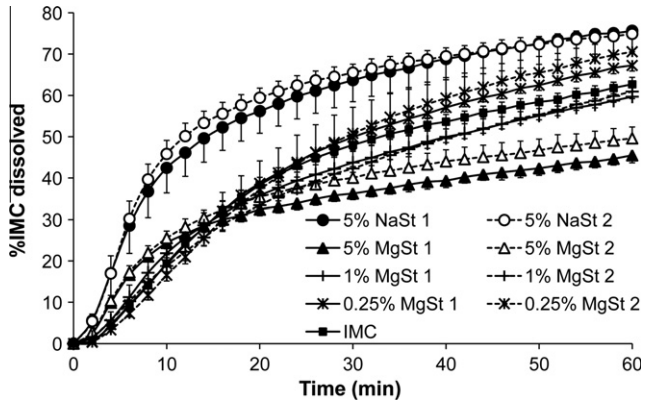

Fig. 4. Dissolution profiles of untreated indomethacin (IMC) and IMC powders mechanofused with magnesium stearate (MgSt; 0.25–5%) and sodium stearate (NaSt; 5%), determined in acetate buffer pH 5.0 using the USP paddle method at 100 rpm and 37 °C (n = 6 for duplicate mixtures).

significant improvements in IMC dissolution ($P > 0.05$). On the other hand, surface coating with 5% NaSt led to further increases in the dissolution rate over the 5% MgSt-IMC sample, with 45.8 ± 3.3% of IMC dissolved after 10 minutes ($P < 0.001$). At 20 min, however, the increasing effect of the mechanofused 5% MgSt-IMC sample on dissolution was no longer evident; the amounts of IMC dissolved between the untreated IMC and all powders mechanofused with MgSt (0.25–5%) were not significantly different ($P > 0.05$). The amount of dissolved IMC for the 5% NaSt-IMC sample remained significantly higher than all other mechanofused samples ($P < 0.001$). At the later stages of the profiles, differences in the dissolution behaviour between the various samples were apparent. Whilst the untreated IMC and samples mechanofused with 0.25% and 1% MgSt were close to 60–70% of dissolved IMC at 60 min, the increase in dissolution seen with the 5% MgSt-IMC sample at earlier times had slowed down considerably and reached an approximate final concentration of 50% dissolved IMC. These observations were not surprising since the strongly hydrophobic nature of MgSt is well known to retard dissolution by decreasing the effective drug-solvent interfacial area [27]. Furthermore, the magnitude of this deleterious effect of MgSt on the later stages of dissolution has been found to be dependent on its concentration [28]. In contrast, the dissolution enhancing effect of a hydrophilic material such as NaSt, demonstrated by higher concentrations of dissolved IMC (75%), could be due to better solvent penetration, thus resulting in greater availability of the drug surface.

4. Discussion

A useful approach to gaining a more profound understanding of the underlying mechanisms during dissolution is to perform mathematical modelling on the dissolution data. The dissolution profiles representing the various mechanofused samples (Fig. 4) were modelled by a non-linear least squares regression analysis with multi-exponential equations. The rationale for the choice of such equations has been the formation of discrete populations of particles, each of which can be described by exponential kinetics; this strategy has been used and described in detail previously [29–32].

To discriminate between the rival models and assess the goodness of fit, a range of statistical parameters obtained using mono-, bi- and tri-exponential equations for the dissolution data of the untreated and mechanofused IMC samples were examined (Table 4). The mono-exponential equation provided very poor fits of the data, producing R^2 values as low as 0.849, small F values (down to 163), as well as high Norm (up to 34.3) and high AIC (ranging from 170–216) values for all samples. However, when the bi-exponential equation was used, a superior data fit was indicated by $R^2 \geqslant 0.995$, markedly larger F values (up to 2725), and substantially lower Norm (in the order of 6.0) and AIC (down to 100) values. Data fitting with the tri-exponential model yielded similar R^2, Norm and AIC values compared to the bi-exponential equation; however, the F values were smaller and the parameter dependencies were equivalent to 1.0, indicating that the model was over-parameterized and that a suitable fit of the data could be achieved using fewer parameters. Thus, the bi-exponential (4 parameter) equation was selected as the best fit equation to describe the dissolution data for all samples.

Table 4
Modelling statistics of multi-exponential equations for dissolution data of the untreated indomethacin (IMC) and IMC powders mechanofused with magnesium stearate (MgSt; 0.25–5%) and sodium stearate (NaSt; 5%).

	R^2	F	Norm	AIC
Mono-exponential (single, 2 parameter)				
IMC	0.961	722	20.9	186
0.25% MgSt	0.981	1491	15.9	170
1% MgSt	0.961	722	18.8	180
5% MgSt	0.849	163	25.3	198
5% NaSt	0.904	274	34.3	216
Bi-exponential (double, 4 parameter)				
IMC	0.995	1862	7.4	128
0.25% MgSt	0.997	2709	6.6	121
1% MgSt	0.997	2725	5.5	110
5% MgSt	0.995	1775	4.6	100
5% NaSt	0.996	2322	6.9	124
Tri-exponential (triple, 6 parameter)				
IMC	0.995	1034	7.4	132
0.25% MgSt	0.997	1505	6.6	125
1% MgSt	0.997	1514	5.5	114
5% MgSt	0.995	986	4.6	104
5% NaSt	0.996	1290	6.9	128

The estimated dissolution parameters (C_d, C_a, k_d and k_a) of the bi-exponential equation for the two replicates of each sample are shown in Table 5. Statistical analysis of the estimated parameters demonstrated no significant differences in all values between the two replicates of each mechanofused sample ($P > 0.05$); differences in the parameter estimates between the various mechanofused samples were then compared. In terms of the dispersed particle distribution, the dissolution rate constant (k_d) for the untreated IMC powder was relatively small (0.045 ± 0.007 min^{-1}). The dissolution rate constant for fully dispersed IMC in dissolution media at pH 5.0 was previously determined to be 0.518 min^{-1} [32]; thus, the "dispersed" particle distribution was primarily constituted of dispersed particles and small agglomerates. Interesting to note was

Table 5
Influence of magnesium stearate (MgSt; 0.25%, 1%, 5%) and sodium stearate (NaSt; 5%) on the estimated bi-exponential modelling parameters [a], for dissolution of indomethacin (IMC) in acetate buffer pH 5.0 (n = 6 for duplicate mixtures).

	C_d (%)	k_d (min^{-1})	C_a (%)	k_a (min^{-1})
IMC [b]	69.9 ± 5.9	0.045 ± 0.007	34.8 ± 5.8	0.001 ± 0.001
0.25% MgSt – 1 [c]	73.4 ± 16.6	0.043 ± 0.015	31.5 ± 15.7	0.003 ± 0.004
0.25% MgSt – 2	79.9 ± 20.2	0.032 ± 0.010	26.0 ± 19.9	0.005 ± 0.010
1% MgSt – 1	36.9 ± 1.1	0.074 ± 0.014	66.2 ± 0.8	0.008 ± 0.001
1% MgSt – 2	39.6 ± 21.5	0.062 ± 0.022	62.9 ± 20.9	0.008 ± 0.004
5% MgSt – 1	30.7 ± 2.3	0.133 ± 0.007	71.7 ± 1.9	0.004 ± 0.000
5% MgSt – 2	35.1 ± 4.1	0.117 ± 0.014	67.2 ± 3.6	0.005 ± 0.001
5% NaSt – 1	54.9 ± 2.9	0.125 ± 0.025	48.7 ± 2.9	0.012 ± 0.003
5% NaSt – 2	64.2 ± 2.3	0.122 ± 0.017	40.3 ± 1.8	0.008 ± 0.001

[a] Estimated parameters for bi-exponential modelling are the initial concentrations of dispersed particles (C_d) and agglomerates (C_a), with their corresponding dissolution rate constants, k_d and k_a.
[b] Untreated IMC data based on one replicate run (n = 6).
[c] IMC powders mechanofused with MgSt (0.25%, 1%, 5%) and NaSt (5%).

an increasing trend in k_d as a function of MgSt concentration, i.e. the k_d increased significantly from mean values of 0.038 ± 0.014–0.068 ± 0.018 to 0.123 ± 0.014 min^{-1} upon mechanofusion of IMC with 0.25%, 1% and 5% MgSt, respectively ($P \leqslant 0.002$). One interpretation of the increasing k_d with increasing MgSt is that the powders were better dispersed as the concentration of MgSt increased leading to a higher dissolution rate due to the increasing surface area. This reasoning was consistent with the fact that the increasing MgSt concentration caused a decrease in the cohesion (Fig. 2B) with resultant less particle interactions and agglomeration. The k_d of the 5% MgSt-IMC sample was significantly higher than all other samples ($P < 0.001$); however, although there was an increasing trend in k_d with MgSt concentration, the k_d of the untreated IMC and samples mechanofused with 0.25% and 1% MgSt were not significantly different ($P > 0.05$). Where k_d were close (i.e. for the uncoated IMC and 0.25% MgSt-IMC sample), the distributions of dispersed particles were likely to be similar. Hence, the estimated initial concentrations of dispersed particles (C_d) between these samples could be directly compared; there was no significant difference in C_d between the untreated IMC and 0.25% MgSt-IMC sample (P > 0.05).

The proportion of initial concentration of agglomerates (C_a) present in each sample seemed to govern the final concentration of dissolved IMC during the later stages of the profiles. Comparison of the dissolution rate constants for agglomerates (k_a) revealed that the agglomerate distributions between the untreated IMC and samples mechanofused with 0.25% and 5% MgSt were not significantly different ($P > 0.05$), as were those between all mechanofused (0.25–5%) MgSt-IMC samples ($P > 0.05$). The significantly higher C_a for the 5% MgSt compared with the untreated IMC and mechanofused 0.25% MgSt samples ($P < 0.001$) manifested in lower concentrations of dissolved IMC (around 50%) at 60 minutes (Fig. 4).

On the other hand, the use of the more water-soluble, surfactant material, NaSt, gave rise to a k_d value which was up to more than three times larger than those of the untreated IMC and mechanofused 0.25% and 1% MgSt samples ($P < 0.001$) and was not significantly different from that of the 5% MgSt-IMC sample (P > 0.05). Comparison between their C_d values revealed that a significantly higher initial concentration of dispersed particles was achieved for the 5% NaSt-IMC sample compared with that for 5% MgSt-IMC ($P < 0.001$). This can be explained by the surface active effect of NaSt that would cause enhanced dispersion of IMC agglomerates in the dissolution medium through increased surface areas [30,33]. This phenomenon can be further supported by a larger agglomerate dissolution rate constant (k_a) and correspondingly lower C_a, which led to a higher final concentration of dissolved IMC (around 75%) (Fig. 4).

On the surface, use of the bi-exponential modelling approach enabled a mechanistic understanding of IMC dissolution occurring from distributions of dispersed and agglomerated particles. The dissolution data can be explained by such a modelling strategy; however, the outcome of this approach was that the dissolution rate constants for 5% MgSt-IMC and 5% NaSt-IMC were similar. Given the contrasting properties of these coating agents, i.e. MgSt was poorly soluble and hydrophobic, while NaSt was more soluble and possesses surfactant properties, the similar magnitude of estimated rate constants was puzzling. Also, the modelling approach was based on dissolution via a diffusion-controlled mechanism, producing approximately exponential dissolution from both dispersed particles and agglomerates.

The highly intensive mechanofusion process was intended to modify the particle surface characteristics through the formation of a coating layer around the IMC powders. Hence, it was appropriate to consider the possibility of a model in which the drug release kinetics of a coated drug particle would be analogous to that of a matrix-diffusion system. The dissolution of IMC from this matrix may be more about diffusion from an intact matrix rather than from a constantly dissolving particle by diffusion through a rate-controlling diffusion layer. The Higuchi model is the most often used mathematical equation to study the release of both water-soluble and poorly water-soluble drugs incorporated in semi-solid and/or solid matrixes [34,35]. This model assumes that the drug is homogeneously dispersed in the planar matrix and the medium into which it is released acts as a perfect sink under pseudo-steady state conditions. In the case of dry coated IMC, the matrix is pure IMC held together by the dry coat with diffusion occurring through the pores in the coat. However, as the IMC (and maybe some of the coat) dissolves, the matrix will collapse and such a model will no longer exist. Following a set of derivations, the model can be simplified to the expression:

$$Q = K_H\sqrt{t} \tag{4}$$

where Q is the concentration of released drug (%), K_H is the Higuchi apparent release rate constant (% $min^{-1/2}$), and t is the release time ($min^{1/2}$). Thus, this model predicts a square root of time dependence of the amount of drug released and an inverse square root of time dependence of the drug release rate.

The comparative dissolution profiles of the untreated IMC and mechanofused samples from 2 to 10 min are shown in Fig. 5A. During the initial stages of dissolution, increases in the amount of drug released were found with increasing concentrations of MgSt. This is counter-intuitive since a thicker hydrophobic surface coating would be expected to reduce the penetration ability of the dissolving medium to the drug particles and hence the dissolution rate. To observe whether there were any distinct differences in the release mechanism with coating level, the same data were then plotted as

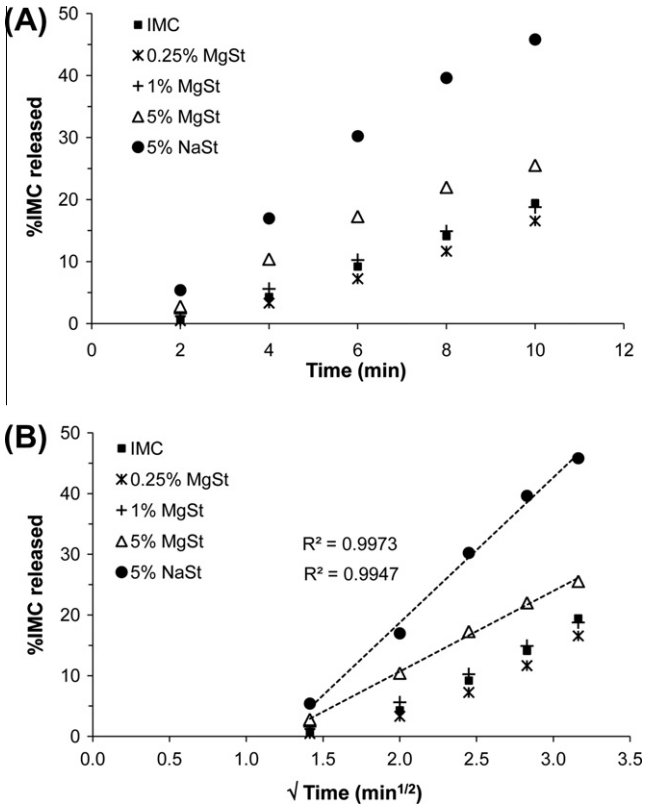

Fig. 5. Concentration of indomethacin (IMC) released (%) for untreated IMC and IMC powders mechanofused with magnesium stearate (MgSt; 0.25–5%) and sodium stearate (NaSt; 5%) plotted as a function of (A) time (min) and (B) square root of time ($min^{1/2}$).

a function of square root of time (Fig. 5B) as described by the simplified Higuchi model (Eq. (4)). The profiles representing the 5% MgSt-IMC and 5% NaSt-IMC mechanofused samples yielded stronger linear correlations with the Higuchi model ($R^2 \geqslant 0.995$) than those of the untreated IMC and mechanofused 0.25% and 1% MgSt samples; this unequivocally indicated the occurrence of a diffusional mechanistic phenomenon. The apparent release rate constants obtained from the slopes of the fitted Higuchi model (Fig. 5B) were 23.9 and 13.3% $min^{-1/2}$ for the samples mechanofused with 5% NaSt and 5% MgSt, respectively. The 1.8-fold higher rate constant of the 5% NaSt-IMC sample demonstrated that diffusional drug release was more rapid than that of the 5% MgSt-IMC sample; as NaSt is a more hydrophilic material than MgSt, this model provided more reasonable estimates of the rate constants than those from the bi-exponential equation that described dissolution occurring from dispersed and agglomerated particles.

A schematic representation of the postulated dissolution mechanisms as deduced from the varying data fits to the Higuchi model is depicted in Fig. 6. The poor fit of the dissolution curves for the untreated IMC and samples mechanofused with 0.25% and 1% MgSt to the Higuchi equation was therefore thought to assume the conventional diffusion-controlled process [36,37]; the drug molecules first detach rapidly from the solid surface to form a saturated solution at the surface, before diffusing through the diffusion layer (formed around the solid) and into the bulk aqueous phase (Fig. 6A). A reasonable explanation for the dissimilar dissolution curves of the 0.25% and 1% MgSt-IMC samples compared to those of the 5% MgSt-IMC might be that at low concentrations, there is insufficient MgSt to retain a continuous film coating around the IMC particles and to maintain the coated particles as a matrix. However, at higher MgSt concentrations, a more continuous, thicker MgSt film was obtained as confirmed by XPS analysis (Table 1). A thicker film layer would increase the separation distance between contiguous primary particles of IMC, hence giving rise to the observed reductions in the intrinsic cohesion and shear stress values at different normal stresses (Figs. 2A and B). This was further corroborated by SEM images that illustrated more dispersible structures following surface treatment of IMC powders with higher concentrations of MgSt (Fig. 3E). Previous literature has also revealed that a concentration of 5% MgSt was optimal for successful coating of micronized particles [38].

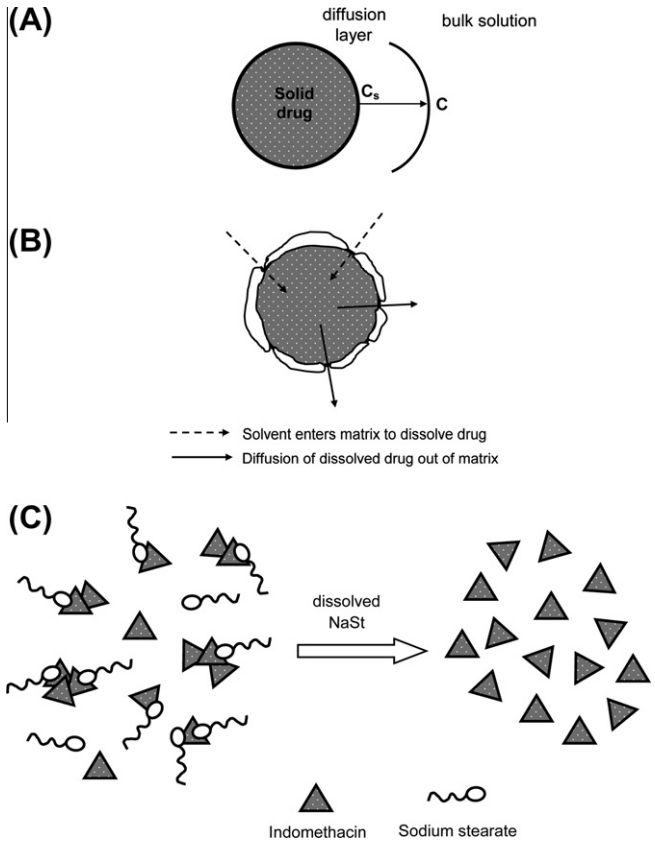

Fig. 6. Schematic mechanistic representations of (A) untreated indomethacin dissolution via a diffusion-controlled process where the drug concentration decreases from C_s (saturated solubility at solid surface) to C (concentration in the bulk solution), (B) initial drug release for mechanofused indomethacin powders from a matrix-diffusion system and (C) enhanced dispersion of indomethacin agglomerates upon mechanofusion with sodium stearate.

In accordance with the Higuchi model, the proportional increases in the amount of drug released with the square root of time for the 5% MgSt and NaSt mechanofused samples suggested drug release from a diffusional-matrix type system [39,40] (Fig. 6B). The FCA coating would form a reservoir (core) that encloses the drug within and upon addition to the dissolution medium, the solvent penetrates the matrix through some of pores present in the coating barrier and dissolves the IMC; the dissolved drug then diffuses out of the matrix for ultimate absorption. This phenomenon would only be operative during the initial stages of dissolution due to the noted non-linear behaviour and systematic increases in the deviations with time past 10 min for these curves. Thereafter, a change in the drug release mechanism would ensue. For MgSt, the pronounced inhibitory effect on IMC dissolution is likely to involve a loss in the integrity of the coating that eventually causes the matrix structure to collapse.

In contrast, the dissolution enhancing effect of the 5% NaSt-IMC sample can be explained by the surface active characteristics of NaSt to cause increased dispersion in the dissolution medium. NaSt is a surfactant, characterized by a negatively charged carboxylate (hydrophilic) head group and a saturated hydrocarbon (hydrophobic) tail group. Based on experimental and theoretical calculations, the critical micelle concentration (CMC) of NaSt in aqueous solution has been determined to be between 4.0×10^{-4} and 5.6×10^{-4} M [41,42]. Considering the molecular mass of 306.46 g/mol, the molar concentration of NaSt in the dissolution medium (1 L) would be 4.9×10^{-7} M at a concentration of 1.5×10^{-5}% w/v, corresponding to the 5% w/w NaSt-IMC mechanofused sample. Therefore, at such low concentrations of NaSt below its CMC, the observed increase in IMC dissolution upon mechanofusion with NaSt would be attributed to a combination of the ability of NaSt to firstly reduce the interfacial tension between the IMC and dissolution medium, hence improving IMC wettability, and secondly enhance dispersion. As illustrated in Fig. 6C, mechanofusion results in the surface adhesion of NaSt monomers onto IMC particles and after rapid dissolution of the soluble NaSt, the high local concentration of surfactant in the microenvironment causes dispersion of the IMC agglomerates. The resulting increased drug surface areas exposed to the dissolution medium manifested in a higher dissolution rate constant (23.9% $min^{-1/2}$) as described by the Higuchi model. Furthermore, this mechanism has previously been observed where surfactants increased the dissolution rate of drugs in interactive mixtures [30,33,43,44].

5. Conclusion

Micronized cohesive powders of indomethacin were dry coated with magnesium stearate (0.25%, 1% and 5%) and sodium stearate (5%) and the dissolution of the poorly water-soluble drug studied. Initially, dissolution of indomethacin increased as a function of magnesium stearate concentration but was later impeded with higher concentrations (5%) of the hydrophobic material. In

contrast, the use of the more hydrophilic sodium stearate enhanced dissolution. Several modelling approaches were used to elucidate the underlying mechanisms during dissolution. The application of a non-linear least squares regression analysis with a bi-exponential equation described the dissolution of mechanofused indomethacin powders occurring from discrete distributions of dispersed and agglomerated particles. However, the unrealistic parameter estimates for the coating materials of contrasting properties were the impetus for considering a diffusional-matrix type system. The Higuchi model adequately described drug release from the 5% sodium stearate and magnesium stearate mechanofused samples by a square root of time relationship. This was indicative that drug release from a matrix-diffusion system was operative in the initial stages of dissolution; thereafter, a change in the mechanism of drug release was apparent. For magnesium stearate, it was postulated that the collapse of the matrix structure gave rise to retardation of indomethacin dissolution. On the other hand, the dissolution enhancing effect of sodium stearate was attributable to its surfactant properties that caused increased dispersion of indomethacin agglomerates through increasing the surface areas available to the dissolution medium. Further investigation into these mechanisms of dissolution would be needed to confirm the observations from this work. In addition, the dissolution of mechanofused indomethacin formulations has only been tested as powders; however, examining the influence of these formulations on the dissolution from other solid dosage forms such as a resulting tablet or capsule form would serve part of a useful future study.

Acknowledgements

Tracy Tay received scholarship support through an Australian Postgraduate Award.

References

[1] J.W. McGinity, C.T. Ku, R. Bodmeier, M.R. Harris, Dissolution and uniformity properties of ordered mixes of micronized griseofulvin and a directly compressible excipient, Drug Dev. Ind. Pharm. 11 (4) (1985) 891–900.
[2] P.A. Hartley, G.D. Parfitt, L.B. Pollack, The role of the van der Waals force in the agglomeration of powders containing submicron particles, Powder Technol. 42 (1985) 35–46.
[3] J. Visser, Van der Waals and other cohesive forces affecting powder fluidization, Powder Technol. 58 (1989) 1–10.
[4] H. Krupp, Particle adhesion theory and experiment, Adv. Colloid Interface Sci. 1 (1967) 111–239.
[5] M. Alonso, M. Satoh, K. Miyanami, Mechanism of the combined coating-mechanofusion processing of powders, Powder Technol. 59 (1989) 45–52.
[6] R. Pfeffer, R.N. Dave, D. Wei, M. Ramlakhan, Synthesis of engineered particulates with tailored properties using dry particle coating, Powder Technol. 117 (2001) 40–67.
[7] J. Yang, A. Sliva, A. Banerjee, R.N. Dave, R. Pfeffer, Dry particle coating for improving the flowability of cohesive powders, Powder Technol. 158 (2005) 21–33.
[8] T. Yokoyama, K. Urayama, M. Naito, M. Kato, T. Yokoyama, The angmill mechanofusion system and its applications, Kona 5 (1987) 59–68.
[9] T. Yokoyama, K. Urayama, T. Yokoyama, Ultra-fine grinding and consequent changes of powder characteristics, Kona 1 (1983) 53–63.
[10] P. Begat, R. Price, H. Harris, D.A.V. Morton, J.N. Staniforth, The influence of force control agents on the cohesive-adhesive balance in dry powder inhaler formulations, Kona 23 (2005) 109–121.
[11] J.N. Staniforth, H. Harris, D.A.V. Morton, R. Bannister, Pharmaceutical compositions for inhalation containing magnesium stearate, WO IPO 0243702 A2 (2002).
[12] M. Kumon, M. Suzuki, A. Kusai, E. Yonemochi, K. Terada, Novel approach to DPI carrier lactose with mechanofusion process with additives and evaluation by IGC, Chem. Pharm. Bull. (Tokyo) 54 (11) (2006) 1508–1514.
[13] P. Begat, D.A.V. Morton, J. Shur, P. Kippax, The role of force control agents in high-dose dry powder inhaler formulations, J. Pharm. Sci. 98 (8) (2009) 2770–2783.
[14] Y. Kawashima, T. Serigano, T. Hino, H. Yamamoto, H. Takeuchi, Effect of surface morphology of carrier lactose on dry powder inhalation property of pranlukast hydrate, Int. J. Pharm. 172 (1998) 179–188.
[15] J.N. Staniforth, Preformulation aspects of dry powder aerosols, in: Proceedings from Respiratory Drug Delivery V, Phoenix, AZ, 1996, pp. 65–74.
[16] T. Ishizaka, H. Honda, M. Koishi, Drug dissolution from indomethacin-starch hybrid powders prepared by the dry impact blending method, J. Pharm. Pharmacol. 45 (1993) 770–774.
[17] T. Ishizaka, H. Honda, K. Ikawa, N. Kizu, K. Yano, M. Koishi, Complexation of aspirin with potato starch and improvement of dissolution rate by dry mixing, Chem. Pharm. Bull. (Tokyo) 36 (7) (1988) 2562–2569.
[18] T. Ishizaka, H. Honda, Y. Kikuchi, K. Ono, T. Katano, M. Koishi, Preparation of drug-diluent hybrid powder by dry processing, J. Pharm. Pharmacol. 41 (1989) 361–368.
[19] K. Nagata, H. Okamoto, K. Danjo, Naproxen particle design using porous starch, Drug Dev. Ind. Pharm. 27 (4) (2001) 287–296.
[20] R.C. Rowe, P.J. Sheskey, M.E. Quinn, Handbook of Pharmaceutical Excipients, sixth ed., Pharmaceutical Press, London, 2009.
[21] A. Dakkuri, H.G. Schroeder, P.P. DeLuca, Sustained release from inert wax matrixes II: Effect of surfactants on tripelennamine hydrochloride release, J. Pharm. Sci. 67 (3) (1978) 354–357.
[22] S. Michielsen, The effect of grafted polymeric lubricant molecular weight on the frictional characteristics of nylon 6,6 fibers, J. Appl. Polym. Sci. 73 (1999) 129–136.
[23] D. Tabor, Mechanism of boundary lubrication, Proc. Roy. Soc. Lond. A. Math. Phys. Sci. 212 (1111) (1952) 498–505.
[24] D.W. Marquardt, An algorithm for least-squares estimation of nonlinear parameters, J. Soc. Ind. Appl. Math. 11 (2) (1963) 431–441.
[25] H.J. Motulsky, L.A. Ransnas, Fitting curves to data using nonlinear regression: a practical and nonmathematical review, FASEB J. 1 (1987) 365–374.
[26] A.C. Shah, A.R. Mlodozeniec, Mechanism of surface lubrication: Influence of duration of lubricant-excipient mixing on processing characteristics of powders and properties of compressed tablets, J. Pharm. Sci. 66 (10) (1977) 1377–1382.
[27] G. Levy, R.H. Gumtow, Effect of certain tablet formulation factors on dissolution rate of the active ingredient III. Tablet lubricants, J. Pharm. Sci. 52 (12) (1963) 1139–1144.
[28] G.K. Bolhuis, C.F. Lerk, H.T. Zijlstra, A.H. de Boer, Film formation by magnesium stearate during mixing and its effect on tabletting, Pharm. Weekbl. 110 (1975) 317–325.
[29] B. Alway, R. Sangchantra, P. Stewart, Modelling the dissolution of diazepam in lactose interactive mixtures, Int. J. Pharm. 130 (1996) 213–224.
[30] J. Liu, P. Stewart, Deaggregation during the dissolution of benzodiazepines in interactive mixtures, J. Pharm. Sci. 87 (12) (1998) 1632–1638.
[31] F.Y. Zhao, P. Stewart, Modeling the deagglomeration of micronized benzodiazepines from powder mixtures added to dissolution media, J. Pharm. Sci. 93 (6) (2004) 1618–1627.
[32] T. Tay, A. Allahham, D.A.V. Morton, P.J. Stewart, Understanding improved dissolution of indomethacin through the use of cohesive poorly water-soluble aluminium hydroxide: Effects of concentration and particle size distribution, J. Pharm. Sci. 100 (10) (2011) 4269–4280.
[33] M. Westerberg, C. Nyström, Physicochemical aspects of drug release XVIII. Use of a surfactant and disintegrant for improving drug dissolution rate from ordered mixtures, STP Pharma Sci. 3 (1993) 142–147.
[34] T. Higuchi, Rate of release of medicaments from ointment bases containing drugs in suspension, J. Pharm. Sci. 50 (10) (1961) 874–875.
[35] T. Higuchi, Mechanism of sustained-action medication. Theoretical analysis of rate of release of solid drugs dispersed in solid matrices, J. Pharm. Sci. 52 (12) (1963) 1145–1149.
[36] H. Grijseels, D.J.A. Crommelin, C.J. de Blaey, Dissolution at porous interfaces VI: Multiple pore systems, J. Pharm. Sci. 73 (12) (1984) 1771–1774.
[37] J.T. Carstensen, M.N. Musa, Dissolution rate patterns of log-normally distributed powders, J. Pharm. Sci. 61 (2) (1972) 223–227.
[38] D. Morton, Dry powder inhaler formulations comprising surface-modified particles with anti-adherent additives, WO 2006/056812 A1, 2006.
[39] T.J. Roseman, W.I. Higuchi, Release of medroxyprogesterone acetate from a silicone polymer, J. Pharm. Sci. 59 (3) (1970) 353–357.
[40] P.I. Lee, Diffusional release of a solute from a polymeric matrix – approximate analytical solutions, J. Membr. Sci. 7 (1980) 255–275.
[41] H.A. Capelle, L.G. Britcher, G.E. Morris, Sodium stearate adsorption onto titania pigment, J. Colloid Interface Sci. 268 (2003) 293–300.
[42] A. Tabazadeh, Organic aggregate formation in aerosols and its impact on the physicochemical properties of atmospheric particles, Atmos. Environ. 39 (2005) 5472–5480.
[43] P.J. Stewart, F.Y. Zhao, Understanding agglomeration of indomethacin during the dissolution of micronised indomethacin mixtures through dissolution and de-agglomeration modeling approaches, Eur. J. Pharm. Biopharm. 59 (2005) 315–323.
[44] P. Stewart, J. Liu, The influence of aggregate microenvironment on the dissolution of oxazepam in ternary surfactant interactive mixtures, J. Pharm. Pharmacol. 54 (2002) 1181–1187.